Closed-Form Analysis of the Abrupt Junction Varactor Doubler

EUGENE W. SARD, FELLOW, IEEE

Abstract—**Circuit equations of the abrupt junction varactor doubler have been consolidated into one implicit equation in one unknown. For tuned input and output circuits, this equation reduces to a cubic equation that is solved explicitly as a function of available input power and circuit loading. Optimum loading conditions for maximum power output are functions of only a single composite parameter.**

For general terminating impedances at input and output frequencies, the consolidated equation is readily solved numerically using the tuned results as a starting point. As examples, doubler frequency responses, with single- and double-tuned load circuits, have been calculated. Surprisingly, double tuning is of limited value in enhancing the instantaneous bandwidth. In addition, for single-tuned load circuits, the frequency response as a function of bias voltage has been calculated, showing the potentiality of greater than 20-percent frequency tunability.

I. Introduction

The ABRUPT junction varactor doubler has received much attention in the literature because of its amenability to analysis [1]–[5], but these analyses have suffered to various degrees from the requirement of the solution of simultaneous equations graphically or on a computer. Furthermore, the analyses have been mostly geared to so-called "full drive" situations and lack the flexibility of readily handling arbitrary power inputs. If the circuit equations could be solved in closed form, it would greatly facilitate doubler analysis including, for example, the determination of instantaneous bandwidth and bias tunability. Such a closed-form solution is described as follows.

II. Derivation of Consolidated Design Equation

Relations for the capacitance c, elastance s, and charge q of the abrupt junction varactor in terms of the junction voltage v (+ is forward bias) are

$$c=\frac{dq}{dv}=\frac{1}{s}=\frac{C_{j0}}{\left(1-\frac{v}{\phi}\right)^{1/2}} \tag{1}$$

$$q=-2\phi^{1/2}C_{j0}(\phi-v)^{1/2}+q_{\phi} \tag{2}$$

where ϕ is the contact potential, C_{j0} is the zero-bias junction capacitance, and q_{ϕ} is the charge at the contact potential. From (1) and (2),

$$q'=-(\phi-v)^{1/2} \tag{3}$$

Manuscript received September 29, 1978; revised December 11, 1978.
The author is with the AIL Division of Cutler–Hammer, Melville, NY 11746.

$$sC_{j0}=-\frac{q'}{\phi^{1/2}} \tag{4}$$

where

$$q'=\frac{q-q_{\phi}}{2\phi^{1/2}C_{j0}}. \tag{5}$$

Also, recasting (3),

$$v=\phi-(q')^2. \tag{6}$$

Consistent with previous analyses [1]–[5], assume no charge components above the second harmonic.

$$q'=Q_0+Q_1e^{j\omega t}+Q_1^*e^{-j\omega t}+Q_2e^{j2\omega t}+Q_2^*e^{-j2\omega t} \tag{7}$$

$$i=\frac{dq}{dt}=I_1e^{j\omega t}+I_1^*e^{-j\omega t}+I_2e^{j2\omega t}+I_2^*e^{-j2\omega t} \tag{8}$$

$$v=V_0+V_1e^{j\omega t}+V_1^*e^{-j\omega t}+V_2e^{j2\omega t}+V_2^*e^{-j2\omega t}+\cdots \tag{9}$$

$$s=S_0+S_1e^{j\omega t}+S_1^*e^{-j\omega t}+S_2e^{j2\omega t}+S_2^*e^{-j2\omega t} \tag{10}$$

where ω is the input angular frequency. From (5), (7), and (8),

$$I_1=j2\phi^{1/2}C_{j0}\omega Q_1 \tag{11}$$

$$I_2=j4\phi^{1/2}C_{j0}\omega Q_2. \tag{12}$$

The equivalent circuit of the varactor junction and external circuitry is shown in Fig. 1. Generally, different varactor series resistances R_{s1} and R_{s2} are shown at input and output frequencies, respectively.

Substitution of (7) and (9) into (6), and the terminal conditions from Fig. 1, give

$$V_0=\phi-(Q_0^2+2|Q_1|^2+2|Q_2|^2) \tag{13}$$

$$V_1=-(2Q_0Q_1+2Q_1^*Q_2)=E_g-(Z_g+R_{s1})I_1 \tag{14}$$

$$V_2=-(Q_1^2+2Q_0Q_2)=-(Z_2+R_{s2})I_2. \tag{15}$$

From (11)–(15), the basic circuit equations are

$$\alpha=2|Q_1|^2+2|Q_2|^2 \tag{16}$$

$$E_g=-2W_1Q_1-2Q_1^*Q_2 \tag{17}$$

$$0=Q_1^2+2W_2Q_2 \tag{18}$$

where

$$\alpha=\phi-V_0-Q_0^2 \tag{19}$$

$$W_1=Q_0-j\phi^{1/2}C_{j0}\omega(Z_g+R_{s1}) \tag{20}$$

$$W_2=Q_0-j2\phi^{1/2}C_{j0}\omega(Z_2+R_{s2}). \tag{21}$$

0018-9480/79/0600-0604$00.75 ©1979 IEEE

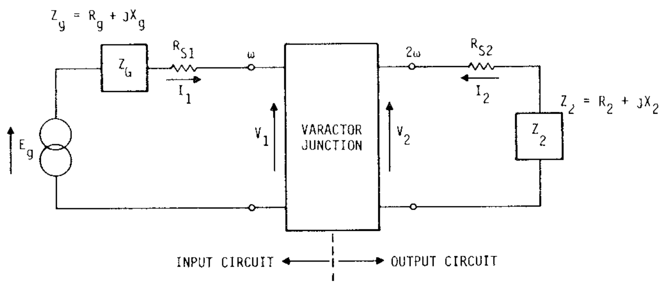

Fig. 1. Equivalent circuit of varactor doubler.

Up to this point, there is nothing essentially different from [1]–[5], but the form of (16)–(18) facilitates the elimination of Q_2 and Q_1. The resulting equation in one unknown (Q_0) is

$$\left(\frac{\alpha(\alpha+2|W_3|^2)}{(P_1)_{av}R_g+4\alpha\,\mathrm{Re}\,[W_2W_3]+8|W_2|^2|W_3|^2}+1\right)^2-\left(1+\frac{\alpha}{2|W_2|^2}\right)=0 \quad (22)$$

where

$$W_3=W_1+2W_2^*. \quad (23)$$

Available input power

$$(P_1)_{av}=\frac{|E_g|^2}{2\,\mathrm{Re}\,[Z_g]}=\frac{|E_g|^2}{2R_g}. \quad (24)$$

A normalized form of (22) is convenient to work with

$$\left(\frac{N}{D}+1\right)^2-\left(1+\frac{\alpha'}{2|w_2|^2}\right)=0 \quad (25)$$

where

$$N=\alpha'[\alpha'+2|w_3|^2] \quad (26)$$

$$D=\frac{R_g}{R_{s1}}\left[\frac{(P_1)_{av}}{P_0}\right]+4\alpha'\,\mathrm{Re}\,[w_2\cdot w_3]+8|w_2|^2\cdot|w_3|^2 \quad (27)$$

$$\alpha'=\frac{\alpha}{\phi}=1-\frac{V_0}{\phi}-(S_0C_{j0})^2 \quad (28)$$

$$P_0=\frac{\phi^2}{R_{s1}}. \quad (29)$$

Equation (25) is the desired consolidated design equation and is a function only of $S_0C_{j0}=-Q_0/\phi^{1/2}$. Also, the quantities w_1, w_2, and w_3 are from (20), (21), and (23):

$$w_1=\frac{W_1}{\phi^{1/2}}=-j\left[\beta\left(\frac{Z_g}{R_{s1}}+1\right)-jS_0C_{j0}\right] \quad (30)$$

$$w_2=\frac{W_2}{\phi^{1/2}}=-j\left[2\beta\gamma\left(\frac{Z_2}{R_{s2}}+1\right)-jS_0C_{j0}\right] \quad (31)$$

$$w_3=\frac{W_3}{\phi^{1/2}}=-j\left[\beta\left(\frac{Z_g}{R_{s1}}+1\right)-4\beta\gamma\left(\frac{Z_2^*}{R_{s2}}+1\right)-j3S_0C_{j0}\right] \quad (32)$$

where

$$\beta=\frac{f}{f_c},\qquad f=\frac{\omega}{2\pi} \quad (33)$$

$$f_c=\frac{1}{2\pi R_{s1}C_{j0}} \quad (34)$$

$$\gamma=\frac{R_{s2}}{R_{s1}}. \quad (35)$$

Note the different definition of f_c in (34) from [1]–[5], which define f_c at reverse breakdown instead of zero bias. Furthermore, note that the phase angle of the bracket in (31) is θ of [1]–[3]; thus the phase angle of w_2 is related to θ by

$$\measuredangle\, w_2=\theta-90°. \quad (36)$$

Examples of the solution of (25) are discussed in Section VI. Once S_0C_{j0} is determined for given circuit and input power values, normalized values of Q_1 and Q_2 can be calculated to complete the solution of (16)–(18):

$$|q_1|=\frac{|Q_1|}{\phi^{1/2}}=|w_2|\left(\frac{2N}{D}\right)^{1/2} \quad (37)$$

$$q_1=\frac{Q_1}{\phi^{1/2}}=\frac{2}{\left(\frac{E_g^*}{\phi}\right)}[\alpha' w_2-|q_1|^2w_3^*] \quad (38)$$

$$q_2=\frac{Q_2}{\phi^{1/2}}=-\frac{q_1^2}{2w_2}. \quad (39)$$

Note, from (24) and (29),

$$\frac{|E_g|}{\phi}=\left[2\left(\frac{R_g}{R_{s1}}\right)\left(\frac{(P_1)_{av}}{P_0}\right)\right]^{1/2} \quad (40)$$

and the phase of any one complex quantity can be arbitrarily chosen.

Two power relations are also of interest. First, is the output power:

$$P_2=2|I_2|^2R_2 \quad (41)$$

which gives

$$\frac{P_2}{P_0}=32\gamma\beta^2|w_2|^2\left(\frac{R_2}{R_{s2}}\right)\left(\frac{N}{D}\right)^2. \quad (42)$$

Second, the power entering the varactor at input frequency is

$$P_{in}=2|I_1|^2R_{s1}+2|I_2|^2(R_2+R_{s2}) \quad (43)$$

which gives

$$\frac{P_{in}}{P_0}=16\beta^2|w_2|^2\left(\frac{N}{D}\right)\left[1+2\gamma\left(\frac{N}{D}\right)\left(1+\frac{R_2}{R_{s2}}\right)\right]. \quad (44)$$

III. Solution Under Tuned Conditions

For tuned input and output circuits,

$$\frac{\beta_0X_{g0}}{R_{s1}}-S_{00}C_{j0}=0 \quad (45)$$

$$\frac{2\beta_0\gamma X_{20}}{R_{s2}} - S_{00}C_{j0} = 0 \text{ (equivalent to } \theta = 0) \quad (46)$$

where additional subscripts 0 on S_0, β, X_g, and X_2 denote values under tuned conditions.

Design equation (25) then reduces to

$$\left(\frac{N_0}{D_0} + 1\right)^2 - \left(1 + \frac{z}{8\beta_0^2\gamma^2 y^2}\right) = 0 \quad (47)$$

where

$$x = \frac{R_{g0}}{R_{s1}} + 1 \quad (48)$$

$$y = \frac{R_{20}}{R_{s2}} + 1 \quad (49)$$

$$N_0 = z\left[z + 2\beta_0^2(4\gamma y - x)^2\right] \quad (50)$$

$$D_0 = \left(\frac{(P_1)_{\text{av}}}{P_0}\right)(x-1) + 8z\beta_0^2\gamma y(4\gamma y - x) + 32\beta_0^4\gamma^2 y^2(4\gamma y - x)^2 \quad (51)$$

$$z = 1 - \frac{V_0}{\phi} - (S_{00}C_{j0})^2 \qquad (\alpha' \text{ under tuned conditions}). \quad (52)$$

Further simplification of (47) leads to a cubic equation in z

$$z^3 + a_2 z^2 + a_1 z + a_0 = 0 \quad (53)$$

where

$$a_2 = 4\beta_0^2 x(4\gamma y - x) \quad (54)$$

$$a_1 = 4\beta_0^4 x^2(4\gamma y - x)^2 - \frac{2(x-1)(3\gamma y - x)\left(\frac{(P_1)_{\text{av}}}{P_0}\right)}{\gamma y} \quad (55)$$

$$a_0 = -(x-1)\left(\frac{(P_1)_{\text{av}}}{P_0}\right)\left[\frac{(x-1)\left(\frac{(P_1)_{\text{av}}}{P_0}\right)}{8\beta_0^2\gamma^2 y^2} + 4\beta_0^2(4\gamma y - x)^2\right]. \quad (56)$$

For given input and output loadings x and y and parameters β_0, γ, and $(P_1)_{\text{av}}/P_0$, (53) can be solved exactly for one positive real root z. There are thus a range of normalized bias voltage V_0/ϕ and corresponding normalized average elastance $(S_{00}C_{j0})$ possible according to (52).

Limitations on these quantities are such that the instantaneous junction voltage v exceeds neither a prescribed forward voltage (ϕ in the case of [1]–[5]) or reverse breakdown voltage V_B. General consideration of the extreme values of v is in the Appendix. Results from [1] are used to determine the extreme values of v for the tuned case in the next paragraph.

$\theta = 0°$ under tuned conditions and the elastance as a function of time from (A-3) is

$$s = S_{00} + 2|S_{10}| \sin \omega_0 t + 2|S_{20}| \sin 2\omega_0 t. \quad (57)$$

From [1, eq. 8.54], extremes of s occur at

$$\cos \omega_0 t_0 = \frac{|S_{10}|}{8|S_{20}|}\left[\left(1 + 32\left|\frac{S_{20}}{S_{10}}\right|^2\right)^{1/2} - 1\right]. \quad (58)$$

The corresponding values of $\sin \omega_0 t_0$ are

$$\sin \omega_0 t_0 = \pm\left[\frac{1}{2}\left(1 + \frac{|S_{10}|}{2|S_{20}|}\cos \omega_0 t_0\right)\right]^{1/2} \quad (59)$$

with the + sign applying for maximum s and minimum v, and conversely for the − sign. From (57) the corresponding normalized extreme values of s are

$$sC_{j0} = S_{00}C_{j0} + 2|S_{10}|C_{j0} \sin \omega_0 t_0\left[1 + 2\left|\frac{S_{20}}{S_{10}}\right| \cos \omega_0 t_0\right] \quad (60)$$

where from (31), (37), (39), and (49),

$$|S_{10}|C_{j0} = \frac{|Q_{10}|}{\phi^{1/2}} = 2\beta_0\gamma y\left(\frac{2N_0}{D_0}\right)^{1/2} \quad (61)$$

$$\left|\frac{S_{20}}{S_{10}}\right| = \left|\frac{Q_{20}}{Q_{10}}\right| = \left(\frac{N_0}{2D_0}\right)^{1/2}. \quad (62)$$

The corresponding extreme values of v from (1) are

$$\frac{v_{\max}}{\phi} = 1 - (s_{\min}C_{j0})^2 \quad (63)$$

$$\frac{v_{\min}}{\phi} = 1 - (s_{\max}C_{j0})^2. \quad (64)$$

It is convenient to express $S_{00}C_{j0}$ in general and $v_{\min}/\phi$ in terms of a specified $v_{\max}/\phi$ and the value of $S_{00}C_{j0}$ for $s_{\min} = 0$ or $v_{\max} = \phi$ (denoted by $S'_{00}C_{j0}$). The latter can be calculated from (60) as

$$S'_{00}C_{j0} = 2|S_{10}|C_{j0} \sin \omega_0 t_0\left[1 + 2\left|\frac{S_{20}}{S_{10}}\right| \cos \omega_0 t_0\right] \quad (65)$$

where the + sign is used in (59) and the other quantities are calculated from (61), (62), and (58). Therefore, in general for any $v_{\max}/\phi$, the normalized tuned average elastance is from (60), (63), and (65),

$$S_{00}C_{j0} = \left(1 - \frac{v_{\max}}{\phi}\right)^{1/2} + S'_{00}C_{j0}. \quad (66)$$

Also, from (64), (60), (59), (65), and (66), the general normalized minimum value of v is

$$\frac{v_{\min}}{\phi} = 1 - \left[\left(1 - \frac{v_{\max}}{\phi}\right)^{1/2} + 2S'_{00}C_{j0}\right]^2. \quad (67)$$

In connection with (66) and (67), it is not thought proper to specify $v_{\max}/\phi = 1$ as in [1]–[5]. A value of $v_{\max}/\phi \approx 0.5$ seems more reasonable in order not to draw excessive forward current, which would violate the assumptions of this analysis and probably result in lowered output power. In any case, once a value of

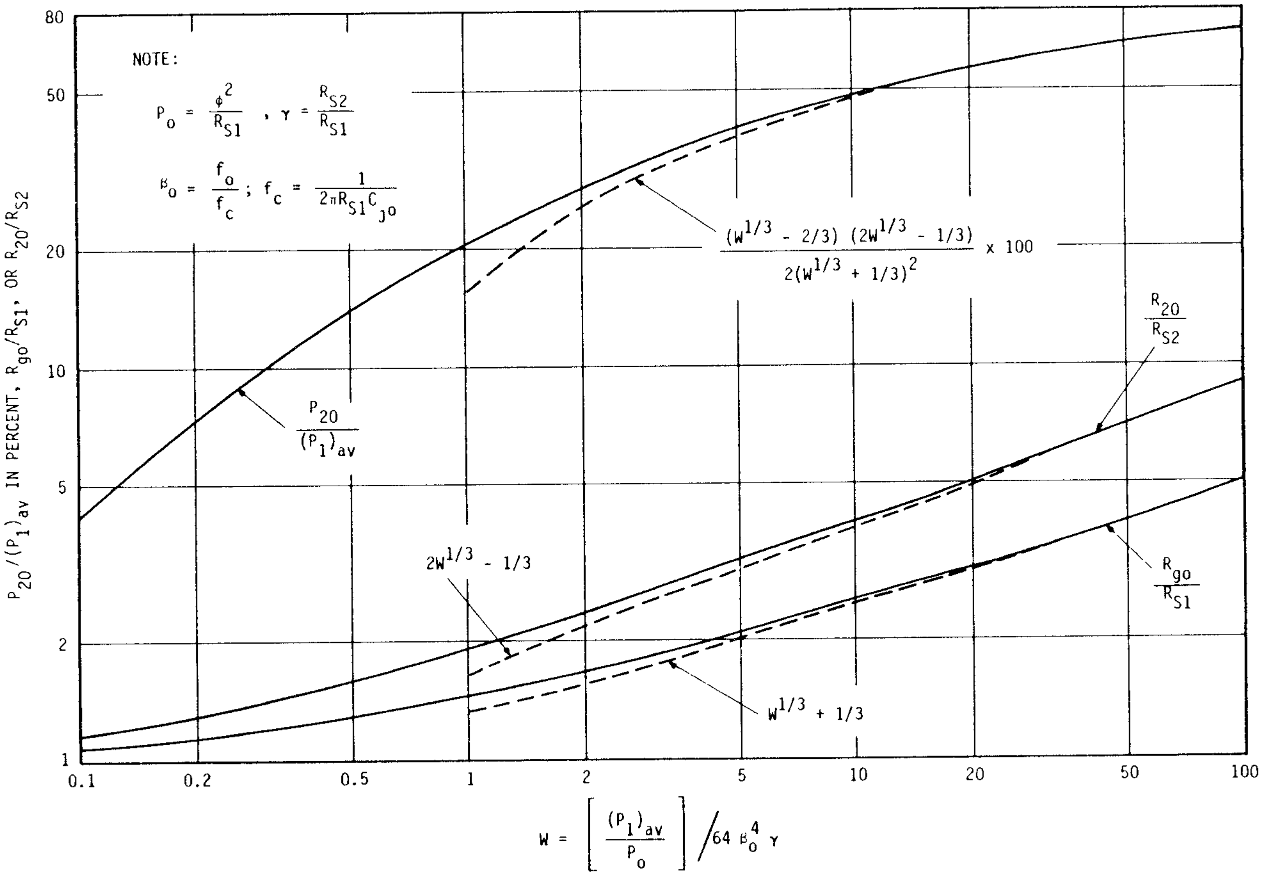

Fig. 2. Optimum abrupt junction varactor doubler design (single composite parameter).

v_{max}/ϕ is specified, (66) and (52) can be used to calculate the normalized dc bias V_0/ϕ. Also, (67) can be used to verify $v_{min} > V_B$ by a safe margin.

Final results of interest in this section are the normalized output and input powers under tuned conditions. From equations (31), (42), (44), and (49), these are

$$\frac{P_{20}}{P_0} = 128\gamma^3\beta_0^4 y^2(y-1)\left(\frac{N_0}{D_0}\right)^2 \tag{68}$$

$$\frac{P_{\text{in }0}}{P_0} = 64\gamma^2\beta_0^4 y^2\left(\frac{N_0}{D_0}\right)\left[1+2\gamma y\left(\frac{N_0}{D_0}\right)\right]. \tag{69}$$

IV. Maximum Output Power and Design Curve

It can be shown that maximum output power for given input and output circuit resistive loadings x and y occurs under tuned conditions. Next, by imposing an input match, $P_{\text{in }0} = (P_1)_{av}$, and simultaneously maximizing the power output, the optimum y is

$$y_{opt} = 2(1+r) \tag{70}$$

where the quantity $r = q_{2opt}/\beta_0$ (q_{2opt} = optimum $Q_{20}/\phi^{1/2}$) is the positive real root of the cubic equation:

$$r(1+r)^2 - w = 0, \qquad w = \frac{\left(\dfrac{(P_1)_{av}}{P_0}\right)}{64\beta_0^4\gamma}. \tag{71}$$

The solution of (71) is

$$r = \left[\frac{w}{2} + \frac{1}{27} + \left(\frac{w^2}{4} + \frac{w}{27}\right)^{1/2}\right]^{1/3} + \frac{1}{9\left[\dfrac{w}{2} + \dfrac{1}{27} + \left(\dfrac{w^2}{4} + \dfrac{w}{27}\right)^{1/2}\right]^{1/3}} - 2/3. \tag{72}$$

The corresponding output efficiency is

$$\frac{(P_{20})_{max}}{(P_1)_{av}} = \frac{r(1+2r)}{2(1+r)^2}. \tag{73}$$

Finally, it can be shown that the normalized tuned input resistance is

$$\frac{R_{\text{in }0}}{R_{s1}} = 1 + \frac{|Q_{20}|}{\phi^{1/2}C_{j0}\omega_0 R_{s1}} = 1 + \frac{q_{20}}{\beta_0}. \tag{74}$$

Therefore, under matched input conditions ($R_{g0} = R_{\text{in }0}$) the optimum x is

$$x_{opt} = 2 + r. \tag{75}$$

It is seen from (70)–(75) that optimum loading conditions are determined by the single composite parameter w. Fig. 2 shows plots of optimum R_{g0}/R_{s1}, R_{20}/R_{s2}, and $P_{20}/(P_1)_{av}$ versus w. Also shown dotted in Fig. 2 are plots

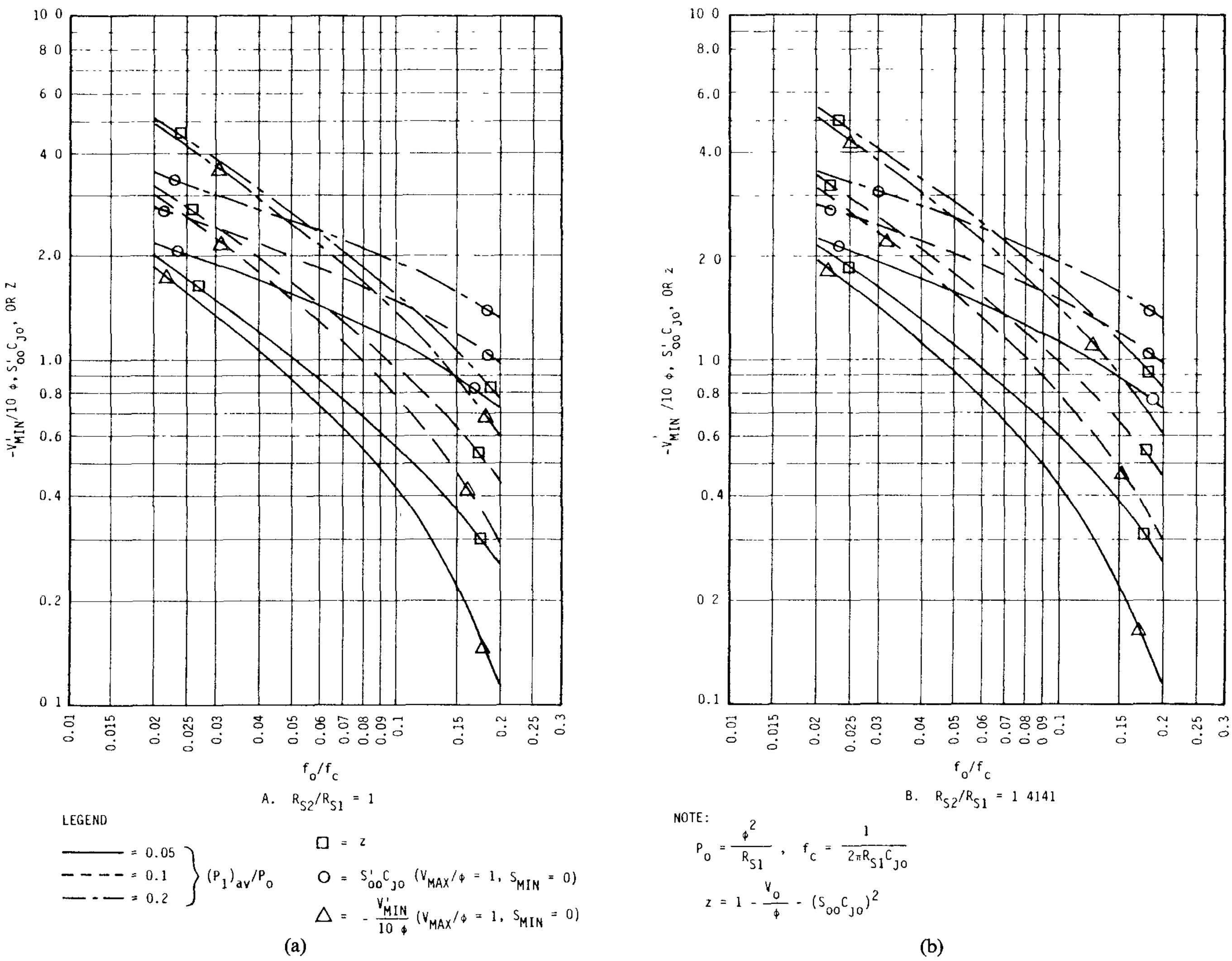

Fig. 3. Optimum abrupt junction varactor doubler design. (a) $R_{s2}/R_{s1}=1$. (b) $R_{s2}/R_{s1}=1.4141$.

from the approximate value of (72):

$$r \approx w^{1/3} - \frac{2}{3}, \qquad w \geqslant 10. \tag{76}$$

Three other optimum relations of interest from (47), (70), (61), and (62) are

$$z_{\text{opt}} = 2\beta_0^2 r\left[r + 8\gamma(1+r)\right] \tag{77}$$

$$\left|\frac{S_{20}}{S_{10}}\right|_{\text{opt}} = \left|\frac{Q_{20}}{Q_{10}}\right|_{\text{opt}} = \frac{1}{2\left[2\gamma\left(1+\frac{1}{r}\right)\right]^{1/2}} \tag{78}$$

$$|S_{10}|_{\text{opt}} C_{j0} = 2\beta_0\left[2\gamma r(1+r)\right]^{1/2}. \tag{79}$$

V. Additional Design Curves and Comparison with [1]

Fig. 3 shows plots for optimum design (maximum output power) of z, $S'_{00}C_{j0}$, and $-v'_{\min}/10\phi$ ($v'_{\min} = v_{\min}$ for $v_{\max} = \phi$) versus $\beta_0 = f_0/f_c$. Fig. 3(a) is for $R_{s2}/R_{s1} = 1$, the case treated in [1]–[5], and Fig. 3(b) is for $R_{s2}/R_{s1} = \sqrt{2}$. The latter might be more appropriate for a millimeterwave doubler, where skin effect could be expected to increase the varactor losses by a factor $\approx\sqrt{2}$ at the output frequency. Interestingly enough, even for $\beta_0 = 0.2$, differences between Fig. 3(a) and (b) are not very great. These curves are plotted from the results of Section III and IV.

It is interesting to make a comparison of Figs. 2 and 3(a) with [1, figs. 8.7–8.9] for particular values of β_0. The following relations are needed to make this comparison (assuming $v'_{\min} = V_B$):

$$\frac{f_0}{f'_c} = \frac{\beta_0}{C_{j0}(s_{\max} - s_{\min})} = \frac{\beta_0}{2S'_{00}C_{j0}} \tag{80}$$

$$\frac{P_{\text{norm}}}{P_0} = \left(1 - \frac{v'_{\min}}{\phi}\right)^2 = (s_{\max}C_{j0})^4 \tag{81}$$

$$\frac{\phi - V_0}{\phi - V_B} = \frac{z + (S'_{00}C_{j0})^2}{1 - \frac{v'_{\min}}{\phi}} \tag{82}$$

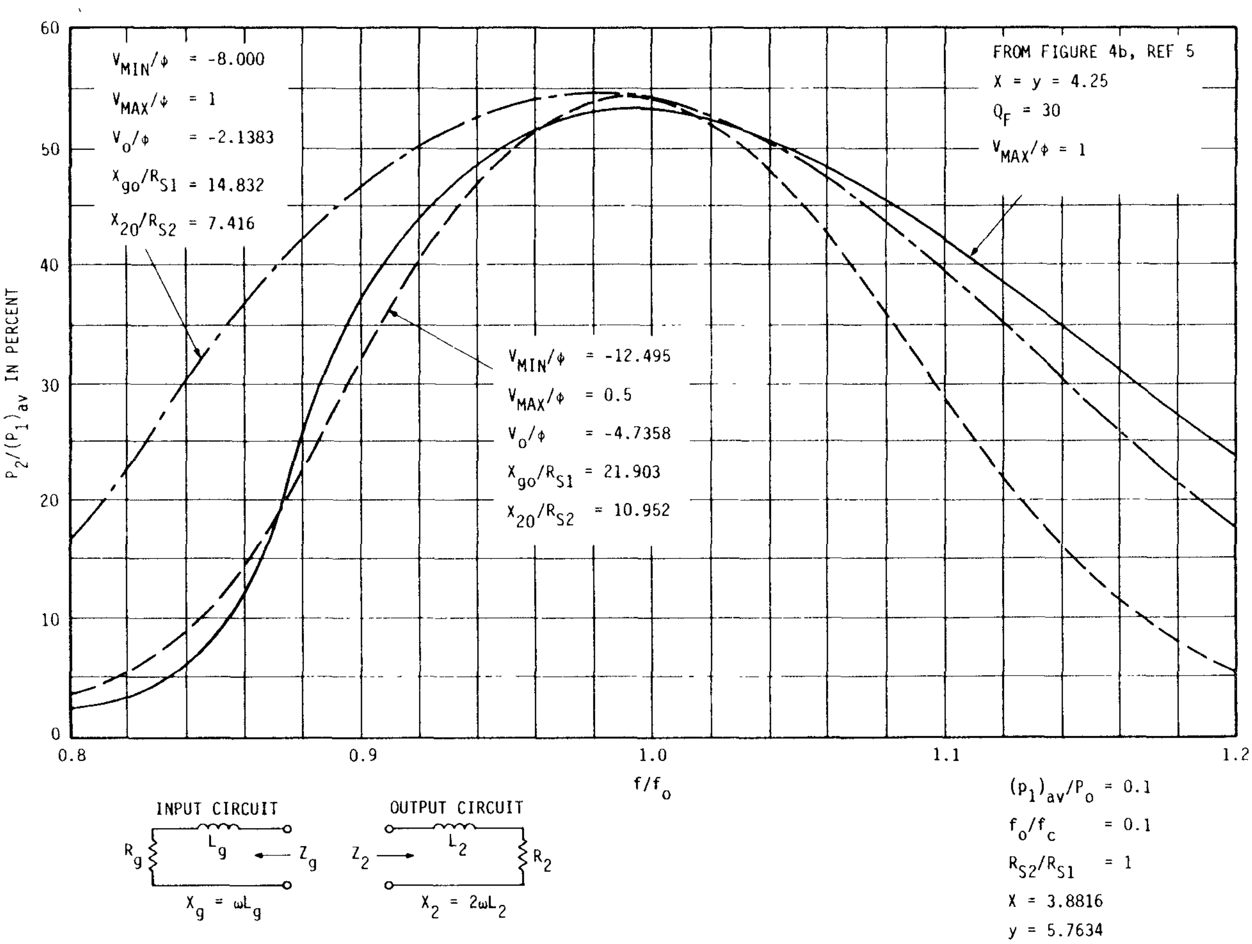

Fig. 4. Theoretical output power versus frequency for lumped single-tuned abrupt junction varactor doubler.

where f_c' and P_{norm} are the cutoff frequency and normalization power defined in [1]. A typical solution plotted on Figs. 2 and 3(a) is for $\beta_0=0.1$, $\gamma=1$, and $(P_1)_{\text{av}}/P_0=0.1$, or $w=15.625$. The corresponding results are $R_{g0}/R_{s1}=2.8816$, $R_{20}/R_{s2}=4.7634$, $z=0.9384$, $S_{00}'C_{j0}=1.4832$, $v_{\min}'/\phi=-7.8001$, and $P_{20}/(P_1)_{\text{av}}=0.53968$. Thus from (80)–(82), $f_0/f_c'=0.0337$, $P_{\text{norm}}/P_0=77.44$, $(\phi-V_0)/(\phi-V_B)=0.3566$, $(P_1)_{\text{av}}/P_{\text{norm}}=1.29\times10^{-3}$, and $P_{20}/P_{\text{norm}}=6.97\times10^{-4}$. The corresponding values scaled off [1, figs. 8.7–8.9] are $P_{\text{in}}/P_{\text{norm}}=1.4\times10^{-3}$, $P_{\text{out}}/P_{\text{norm}}=8.3\times10^{-4}$, $R_{\text{in}}/R_s=3.0$, $R_2/R_s=3.5$, and $(V_0+\phi)/(V_B+\phi)=0.353$, which is only fair agreement.

VI. Examples of Calculation of Instantaneous Bandwidth and Bias Tunability

The performance of the doubler versus frequency and/or dc bias can be calculated from (25)–(44) as described in Section II provided S_0C_{j0} is first calculated at each frequency. It has been found that starting from the tuned condition value $S_{00}C_{j0}$, a simple binary search for S_0C_{j0} to satisfy (25) is easily accomplished with the HP 9820A calculator, for example. Additional calculations for each new frequency can similarly be made starting from the result of the just previous calculation if the frequency increment is not too great. The results for typical lumped single-tuned input and output circuits are plotted in Fig. 4. Two responses are shown, one for $v_{\max}/\phi=1$ (an unrealistic value as mentioned in Section III) for comparison with [5] and the other for $v_{\max}/\phi=0.5$. It is seen that the former has an instantaneous bandwidth advantage due to its lower Q input and output circuits. Also shown is a copy of the plot for $Q_F=30$ (equivalent to $f_0/f_c'=0.0333$) in [5, fig. 4(b)]. The difference in shape of the latter and the plot for $v_{\max}/\phi=1$ may be due to inaccuracies arising from slow convergence of numerical solutions; the use of equal input and output loading in [5] $(x=y\approx4.25)$ has only a very small effect on the shape of the plot.

The effect of lumped double tuning on the circuit response $(v_{\max}/\phi=0.5)$ is shown in Fig. 5. The single-tuned plot of Fig. 4 is repeated for reference, and four plots of different degrees of double tuning of the input and output circuits are shown. Unexpectedly, in view of [2], double tuning increases the instantaneous bandwidth only slightly, and only for double tuning of the input circuit. Greater amounts of input circuit double tuning than that shown do not increase the bandwidth. Nonoptimum loading in conjunction with double tuning may increase the bandwidth more at the price of reduced

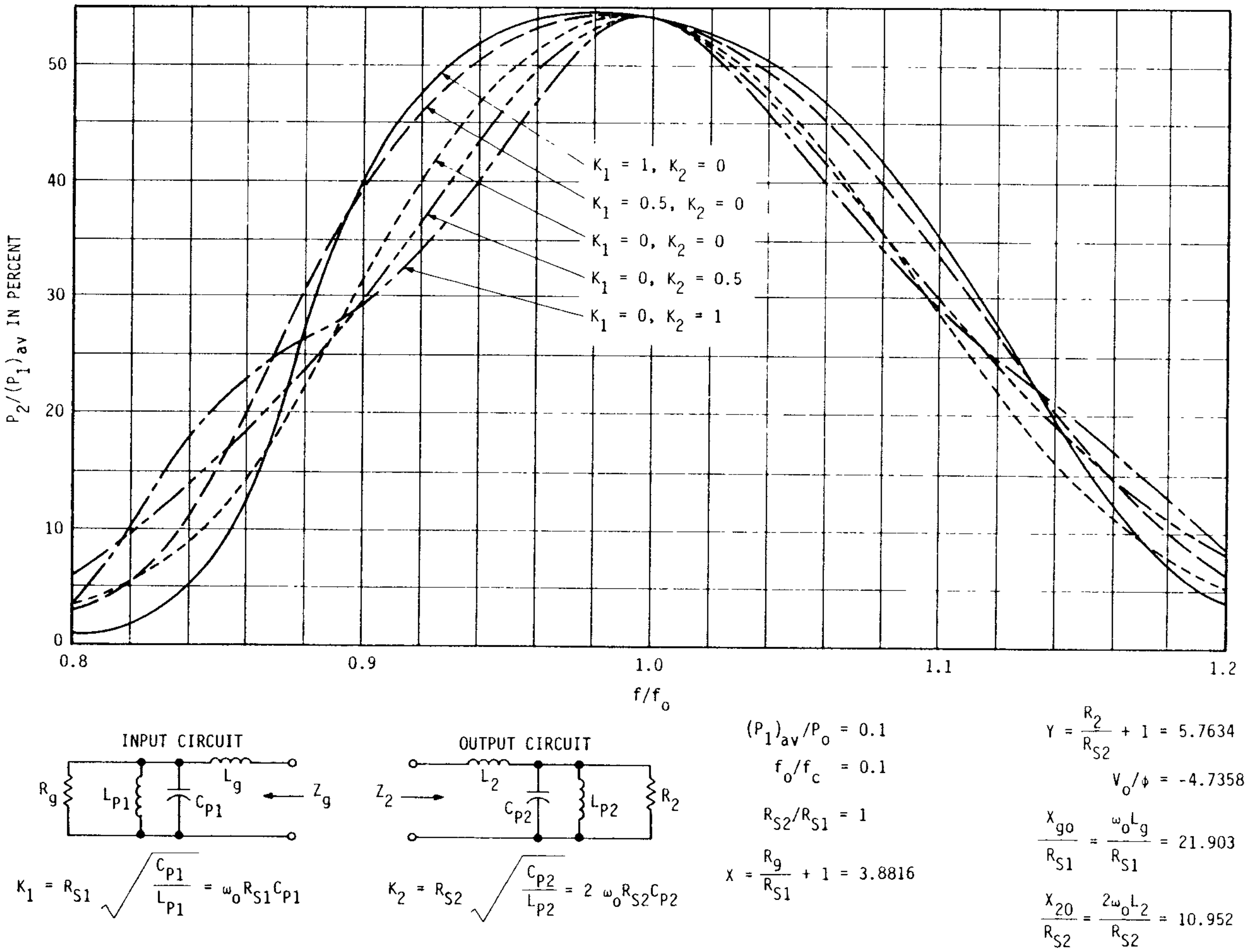

Fig. 5. Theoretical output power versus frequency for lumped double-tuned abrupt junction varactor doubler.

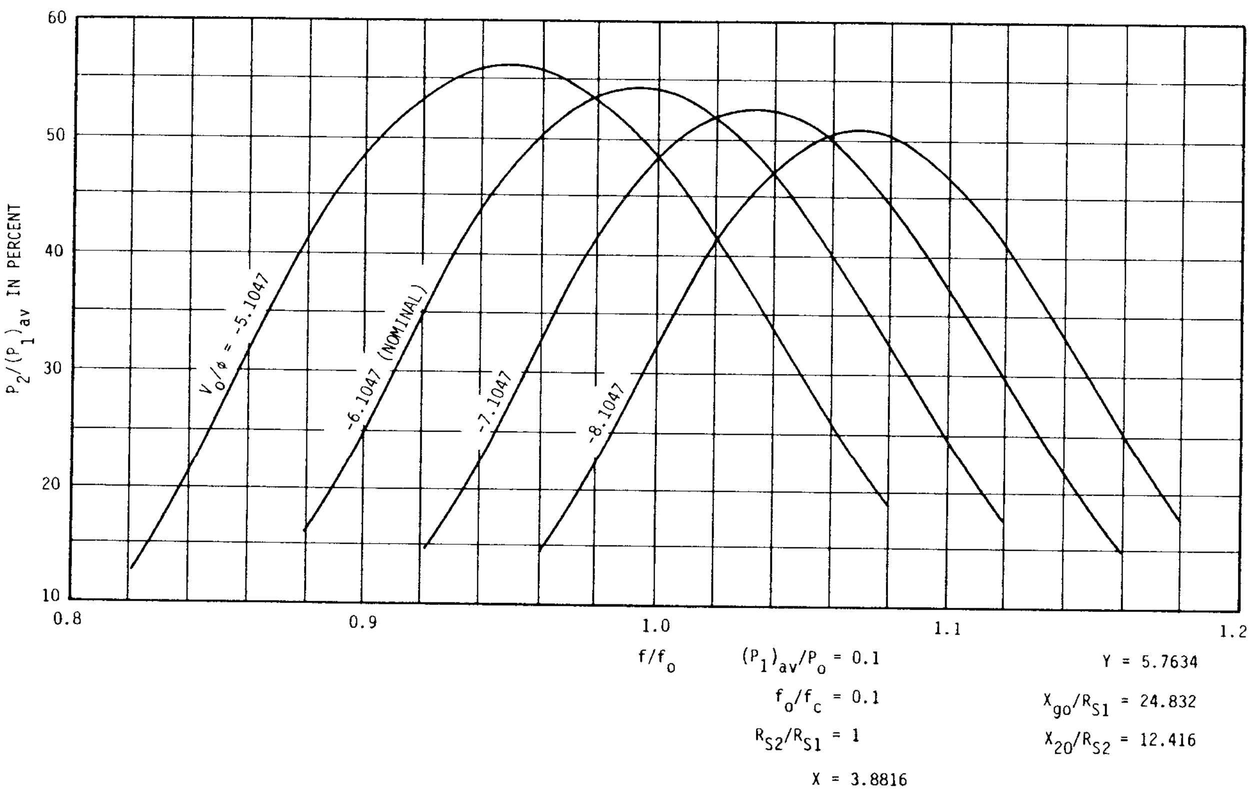

Fig. 6. Theoretical output power versus frequency and bias voltage for lumped single-tuned abrupt junction varactor doubler.

midband efficiency, as also mentioned in [2], but this was not investigated.

Fig. 6 shows an example of the relatively large bias tunability predicted. Qualitatively, this arises because the output circuit tuning tends to track the input circuit tuning as the bias is varied. The nominal design was for $v_{max}/\phi=0$, resulting in $V_0/\phi=-6.1047$ for the parameters shown in the figure. For $\Delta V_0/\phi=1$, $v_{max}/\phi<0.48$ and $v_{min}/\phi>-13.31$. The corresponding values for $\Delta V_0/\phi=-2$ are -0.99 and -17.52. These untuned voltage extreme values were calculated using the iterative procedure described in the Appendix. In practice, by initially starting at the tuned values of ωt_0 for extreme values of v and subsequently using the just previously calculated values of ωt_0, it was not necessary to refer to [2].

VII. Summary and Conclusions

Analysis of the abrupt junction varactor doubler is greatly facilitated by consolidation of the circuit equations into one equation in one unknown. For tuned input and output circuits, the equation reduces to a cubic equation that can be solved exactly. In contrast with previous analyses, calculations are made for arbitrary specified available input power levels instead of principally for "full" drive between reverse breakdown and contact potential. The calculations also consider possibly higher varactor losses at the output frequency compared to those at the input frequency. An interesting result under tuned conditions is that for given input and output resistive loadings, a unique output power results, but a range of dc bias voltages is possible.

The tuned condition is optimum for maximum power output, and optimum loading conditions are derived that are functions of a single composite parameter only. These optimum loading conditions differ slightly from those of [1] and [4], but the resultant power outputs are essentially the same for typical equivalent numerical examples.

For general terminating impedances at input and output frequencies, the consolidated equation can be solved numerically (with a simple program on the HP 9820A calculator, for example) using the tuned results as a starting point. Consequently, predictions of instantaneous bandwidth and bias tunability are readily made for given circuit configurations. Analysis of lumped circuit configurations leads to the surprising conclusion that double tuning is of limited value in enhancing the instantaneous bandwidth, and then only for double tuning of the input circuit. Another result is that bias tuning offers the possibility of wide tunability of the output response.

Appendix
Extreme Values of v in General

The extreme values of v can be calculated from the extreme values of s using (63) and (64). In general, the elastance from (10) is

$$s=S_0+2|S_1|\cos(\omega t+\theta_1)+2|S_2|\cos(2\omega t+\theta_2) \quad \text{(A-1)}$$

where θ_1 and θ_2 are the phase angles of S_1 and S_2. From (39), (4), (7), (10), and (36), θ_2 and θ_1 are related by

$$\theta_2=2\theta_1+90°-\theta. \quad \text{(A-2)}$$

Choose $\theta_1=-90°$ without loss of generality and consistent with [2] and [3]. Then (A-1) reduces to

$$s=S_0+2|S_1|\sin\omega t+2|S_2|\sin(2\omega t-\theta). \quad \text{(A-3)}$$

Extremes of s occur at ωt_0 such that

$$f(\omega t_0)=\cos\omega t_0+\rho\cos(2\omega t_0-\theta)=0 \quad \text{(A-4)}$$

where

$$\rho=2\left(\frac{|S_2|}{|S_1|}\right). \quad \text{(A-5)}$$

Rough solutions of (A-4) can be derived from $\omega t_0=\psi_A$ (for s_{max}) and $\omega t_0=\psi_B$ (for s_{min}) of [2, fig. 2] (parameter $u=\rho^2$). More exact solutions can be calculated from Newton's method, starting at estimated values from [2, fig. 2] to avoid converging on spurious solutions.

$$(\omega t_0)_{n+1}=(\omega t_0)_n+\frac{\cos(\omega t_0)_n+\rho\cos\left[2(\omega t_0)_n-\theta\right]}{\sin(\omega t_0)_n+2\rho\sin\left[2(\omega t_0)_n-\theta\right]}. \quad \text{(A-6)}$$

The extreme values of s can then be calculated from (A-3) using the appropriate values of ωt_0 from (A-6).

Acknowledgment

The simple optimum loading results of Section IV were first derived by D. Breitzer of AIL using a waveform approach. The present analysis was then manipulated to give the same results.

References

[1] P. Penfield, Jr. and R. P. Rafuse, *Varactor Applications*. Cambridge, MA: MIT Press, ch. 8, 1962.
[2] A. I. Grayzel, "The bandwidth of the abrupt-junction varactor-frequency doubler," *IEEE Trans. Circuit Theory*, vol CT-13, pp. 52–58, Mar. 1966.
[3] ——, "Computation of the performance of the abrupt junction varactor doubler," *IEEE Trans. Microwave Theory Tech.*, vol MTT-14, pp. 239–242, May 1966.
[4] J. O. Scanlan and P. J R. Laybourn, "Large signal analysis of varactor harmonic generators without idlers," *Proc. Inst. Elec. Eng.*, vol. 112, no. 8, pp. 1515–1522, Aug. 1965.
[5] ——, "Bandwidth in varactor harmonic generators," *Proc. Inst. Elec. Eng.*, vol. 114, no. 7, pp. 887–893, July 1967.